Reconfigurable liquid pumping in electric-field-defined virtual microchannels by dielectrophoresis†

Shih-Kang Fan,* Wen-Jung Chen, Tin-Hsu Lin, Tsu-Te Wang and Yen-Chen Lin

Received 15th January 2009, Accepted 18th February 2009
First published as an Advance Article on the web 9th March 2009
DOI: 10.1039/b900790c

Dielectrophoresis (DEP), widely used to generate body forces on suspended particles, is investigated to provide surface forces at the liquid–medium interfaces and pump a high-permittivity liquid in a low-permittivity medium along a virtual microchannel defined by an electric field between parallel plates. Because the pumping pressure is proportional to the square of the intensity of the electric field and independent of the channel width, DEP pumping is advantageous as the dimension of the microchannel shrinks down. The absence of the channel walls simplifies the fabrication processes and further increases its feasibility in nanofluidic applications. We demonstrate water pumping in an immiscible silicone oil medium at adjustable velocities by applying voltages above the threshold value whose square is linearly proportional to the cross-sectional aspect ratio (AR), *i.e.*, the height to width ratio, of the microchannel. With a properly designed AR, liquid valve is achieved by appropriate voltage applications. Without the barriers of channel walls, merging multiple streams and capillary filling of the spacing between electric-field-defined virtual microchannels are observed and studied. Moreover, *in situ* reconfigurable liquid pumping is demonstrated by a four way switching valve on a programmable crossing electrode set.

Introduction

Pumping liquids in microchannels is essential to the study of microfluidics[1] and practical to wide applications, including lab-on-a-chip (LOC).[2,3] Various microfabrication techniques have been developed to carve and seal microchannels on silicon, glass, or polymer substrates.[4–6] To drive liquids in microchannels, different pumping mechanisms have been investigated. For example, mechanical micropumps transport liquids through hydraulic pressure differences, while non-mechanical electroosmotic pumping[7,8] relies on the zeta potential on the channel wall and electric potential difference across the liquid in a microchannel. Although the microfabricated physical channel walls assist pumping in mechanical or/and electrical way(s) as described above, they eliminate the controllability of the liquid streams during the operation of different applications.

Guiding liquids without channel walls is an approach to realize reconfigurable microchannel networks. Previously, pumping liquid within "virtual" walls determined by the hydrophobic–hydrophilic boundaries has been demonstrated on a self-assembled monolayer (SAM) modified surface.[9] However, the position and the strength of the boundaries were not easily altered during operation; while surface-tension-defined channel walls limited the maximum pumping pressure provided off-chip and consequently the maximum liquid velocity. Alternatively, taking advantage of laminar flow, the direction and shape of a core stream of sandwiched streams have been manipulated by the sheath streams for sample preparation[10] and liquid lens[11] applications. The flexibility of the core stream was still constrained by the relative flow rates and the design of the channel walls confining the whole sandwiched streams. Here we report liquid pumping in an electric-field-defined microchannel with more robust and controllable virtual channel walls, which are electrically reconfigured *in situ* to yield adjustable stream directions and shapes. In addition to determining the boundaries of the virtual microchannel, the electric field drives the liquid on the energized electrode patterns between parallel plates by dielectrophoresis (DEP); hence, off-chip pumps are not required.

Principle

DEP has been widely employed to manipulate polarizable particles, including nucleic acids, proteins, cells, and nanoparticles, in liquids by non-uniform electric fields.[12–15] In addition to acting on suspended particles, DEP has been investigated to drive liquids in discrete (droplet) and continuous (bulk) forms. On the one hand, analogous to suspended particles, liquid droplets were driven in immiscible fluid media by DEP.[16,17] On the other hand, DEP provides surface forces to continuously draw liquids of higher permittivity along a strong electric field into the region of lower permittivity, *e.g.*, air.[18–27] For example, Pellat demonstrated the rise of dielectric liquid by application of a DC voltage between a pair of electrode plates dipped vertically into a dish full of the dielectric liquid by macroscopic apparatus.[18,19] The height-of-rise was experimentally and theoretically explained by force balance between the gravity body force and the DEP surface force in the direction normal to the liquid. The normal stress (or force density) caused by DEP acting from the

Institute of Nanotechnology, National Chiao Tung University, 207, Engineering 1, 1001 University Road, Hsinchu, Taiwan. E-mail: skfan@mail.nctu.edu.tw; Fax: +886 3-5729912; Tel: +886 3-5712121 ext 55813

† Electronic supplementary information (ESI) available: Movies. See DOI: 10.1039/b900790c

dielectric liquid to air is $\varepsilon_0(\varepsilon_L - \varepsilon_M)E^2/2$, where E is the electric field intensity, ε_0 (8.85×10^{-12} F m^{-1}) is the permittivity of the vacuum, and ε_L and ε_M are the relative permittivities of the liquid and medium (in this case, air), respectively.[20] Therefore, by applying V between W wide parallel electrode plates spaced d apart, the DEP force is:

$$F = \frac{\varepsilon_0(\varepsilon_L - \varepsilon_M)W}{2d} V^2 \quad (1)$$

Based on the experiments of height of rise, researchers have demonstrated an electric siphon and proposed a wall-less pipe by DEP.[21,22]

More recently, similar to dielectric liquids, Jones *et al.* drove aqueous liquids against gravity by an AC electric field between parallel electrode plates coated with dielectric layers to eliminate electrochemical reactions between the aqueous liquid and the electrodes.[23–25] Because the electrodes were covered by a layer of dielectric material, when applying a low frequency signal between the electrodes, electrowetting-on-dielectric (EWOD) occurred. Hence high frequency signals were necessary to make the signal penetrate the dielectric and generate E across the liquid and to achieve DEP by dielectric-coated electrodes. The frequency effect was detailed in the literature.[23–25] Furthermore, with microfabricated coplanar electrodes covered by a dielectric layer, aqueous liquid columns were drawn along the electrode pair from a droplet dispensed on an open surface by DEP.[26] Reliable forming and dispensing of picolitre droplets was also demonstrated.[27]

In this paper, following the studies of overcoming gravity between plates, forming liquid columns on an open surface, and wall-less pipes, DEP is developed as a stable pumping mechanism for continuous flow microfluidics: aqueous liquids are pumped horizontally in an immiscible fluid medium between parallel plates by patterned electrodes. As shown in Fig. 1(a), a pumped liquid is surrounded by a medium between plates. When applying an appropriate electric signal V between the top blank electrode and the bottom patterned electrode, the electric field between the electrodes generates a DEP force at the liquid–medium interface and pulls the liquid along the electrode pattern, resulting in liquid pumping in an electric-field-defined virtual microchannel. Cross-sectional configuration of the device (Fig. 1(b)) presents its simplicity comparing with most continuous flow microfluidic devices requiring channel walls. For the existence of the dielectric layer, signals of high frequencies are necessary for DEP. It is helpful to realize if a frequency is sufficient for DEP by using the cutoff frequency (f_C) of the device whose simplified equivalent circuit consists of resistors and capacitors. If the frequency is much higher than the f_C ($f \gg f_C$), the DEP pumping force in the W wide and d high virtual microchannel can be approximated by eqn (1), and interfacial pressure difference across the liquid–medium interface caused by the DEP surface force density is:

$$\Delta P = P_M - P_L = \frac{\varepsilon_0(\varepsilon_L - \varepsilon_M)}{2} E^2 \quad (2)$$

In this study, we applied 100 kHz signals to pump water by DEP in a 25 and 50 μm high gap between parallel plates. Based on our previous studies,[26] the f_C of such a parallel-plate device containing water is ~11.6 kHz when d is 25 μm and ~7.8 kHz when d is 50 μm, obtained from the resistance and the capacitance of the pumped liquid (water) and the capacitance of the dielectric layer (SU-8). To simplify the calculations of the DEP force and the interfacial pressure difference, we assume that 100 kHz is sufficient to neglect the voltage drop across the dielectric layer causing EWOD and simply use eqn (1) and (2) for the analyses. Exact DEP force and interfacial pressure differences, which are functions of the frequency, can be derived from closed surface integral of the Maxwell stress tensor.[23–25]

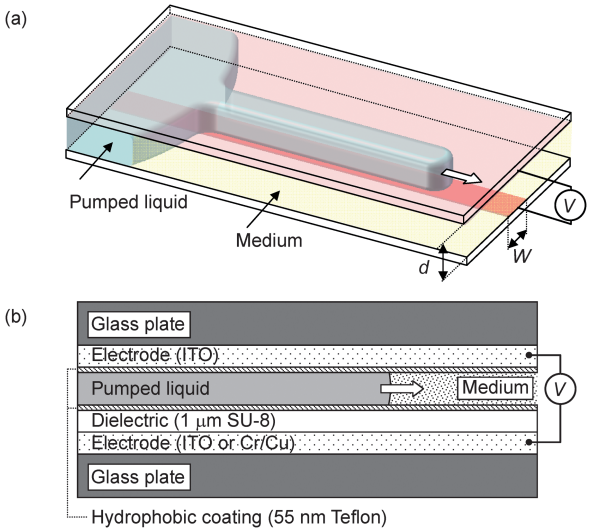

Fig. 1 Principle of DEP pumping. (a) Sketch of DEP pumping between parallel plates in an electric-field-defined virtual microchannel whose cross-sectional aspect ratio (AR = d/W) is determined by the channel height (d) and the electrode width (W). By applying V between the top unpatterned electrode and the bottom patterned electrode, high-permittivity liquid can be pumped along the electrode pattern in a low-permittivity medium. (b) Configuration of the device. Top glass plate was covered by blank ITO and Teflon (AF 1600, DuPont) layers. Bottom glass plate contained patterned electrode(s), dielectric (SU-8 2002, MicroChem), and Teflon layers.

Experiment

Sample preparation

As shown in Fig. 1(b), a pumped liquid is surrounded by a medium and squeezed between parallel plates. To achieve a stable and efficient model system, de-ionized water and silicone oil were chosen as the pumped liquid and the medium, respectively. Silicone oil ($(CH_3)_3SiO[SiO(CH_3)_2]_nSi(CH_3)_3$, Dow Corning 200® Fluid, $\varepsilon_M = 2.5$) was used to eliminate evaporation, while water was selected because of its high relative permittivity ($\varepsilon_L = 80$) resulting in a larger DEP force. However, other combinations of the fluids are possible if the pumped liquid owns a higher permittivity than that of the medium. For example, we observed water or silicone oil pumping in air, which is fundamentally similar as the height-of-rise experiments for aqueous and dielectric liquids in air mentioned above.

Glass plates were used for observation (top plate) and electric isolation (bottom plate) purposes. The bottom glass plate contained patterned electrodes to establish the strong electric field region(s) by appropriate voltage applications. The pumped

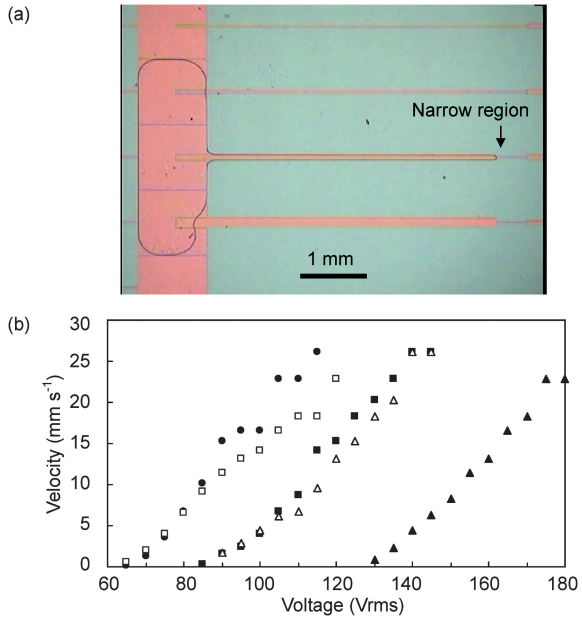

Fig. 2 Pumping velocity measurements. (a) An array of linear electrodes (Cu/Cr) with different widths was patterned on the bottom plate. De-ionized water was pumped in silicone oil (200® Fluid, Dow Corning) along a 100 μm wide and 50 μm high (AR = 0.5) microchannel until the narrow region of the electrode at an average velocity of 1.3 mm s^{-1} when applying a 70 Vrms and 100 kHz signal. Video 1 can be seen in the ESI.† (b) Pumping velocity *versus* applied voltage; ●: AR = 50 μm/100 μm = 0.5, ■: AR = 50/50 = 1, ▲: AR = 50/25 = 2, □: AR = 25/50 = 0.5, △: AR = 25/25 = 1.

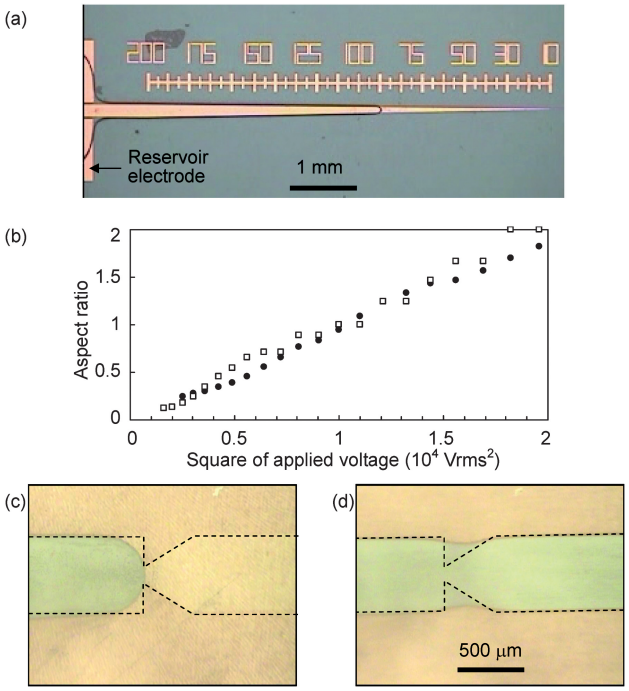

Fig. 3 Voltage-controlled valve. (a) Pumping water in oil on a tapered electrode (Cu/Cr) with a decreased width from 200 μm to 10 μm. When 80 Vrms was applied between the 50 μm high channel, water was successfully pumped until the channel width became ~90 μm where the AR was 0.56. In other words, to achieve 0.56 AR, the threshold voltage was 80 Vrms. Video 2 can be seen in the ESI.† (b) Measured AR plotted against the square of the applied voltage in 50 μm high (●) and 25 μm high (□) channels. (c) The pumped liquid was stopped before the notch when insufficient voltage was applied. The width of the notched ITO electrode was 500 μm in the wide region and 100 μm in the narrow region. (d) When sufficient voltage was applied, liquid passed the notch.

liquid, *i.e.*, water, of higher permittivity was attracted by the strong electric field in the oil medium of lower permittivity. Different electrodes were designed and tested, including linear (Fig. 2(a)), tapered (Fig. 3(a)), notched (Fig. 3(c) and (d)), meandered (Fig. 4), and crossing (Fig. 5) electrodes. The electrode patterns were fabricated by wet etching an ITO (200 nm thick) or Cu/Cr (150/20 nm thick) conductive layer deposited on the bottom glass plate by diluted *aqua regia* solution (NNO_3 : HCl : H_2O = 1 : 3 : 6 at 40 °C) or CR-7T (Cyantek), respectively. A 1 μm thick SU-8 (SU-8 2002, MicroChem) was subsequently spun on the patterned electrodes as a dielectric layer on the bottom plate. To facilitate liquid handling, 55 nm thick Teflon (AF 1600, DuPont) was spun. The top glass plate contained a layer of unpatterned ITO covered by Teflon.

Before testing, a specified volume of water was first dispensed on the bottom plate where spacers of proper thicknesses were attached. The top plate was carefully assembled onto the spacers on the bottom plate. An adequate amount of silicone oil was then injected to fill the gap between the parallel plates as the medium. The driving signals were connected to the electrodes *via* switches controlled by the LabVIEW software.

Linear electrode (pumping velocity)

As described by eqn (1), the DEP force is dependent on not only the applied voltage (V) but also the width (W) and height (d) of the virtual microchannel. To evaluate the pumping ability of DEP, the pumping velocities of water in oil was first tested. An array of linear electrodes with different widths was patterned on the bottom plate (Fig. 2(a)) to provide different W. Meanwhile, the d was adjusted by using different spacers of desirable thicknesses. 100 kHz signals with varied voltages were applied on one of the linear electrodes to pump water along the length of the electrode until a narrow region of the electrodes for 6.1 mm. Pumping velocity was measured by observing the advancing meniscus from recorded videos. For example, it took 4.7 s (Video 1 in the ESI†) to pump water in a 100 μm wide (W) and 50 μm high (d) virtual microchannel, whose cross-sectional aspect ratio (AR = d/W) was 0.5, until a 15 μm wide narrow region (Fig. 2(a)) when 70 Vrms was applied. The average velocity was calculated as 1.3 mm s^{-1}. Limited by the video frame rate (30 frame s^{-1}), average velocities below 30 mm s^{-1} were measured and plotted in Fig. 2(b), while higher velocities were attainable as can be seen in Video 1 in the ESI.†

To obtain accurate pumping velocity, it was necessary to keep the reservoir from moving. Because the inner surfaces of the parallel plates were coated by Teflon, the position of the reservoir would be influenced when the DEP force is larger than the friction force of the reservoir mainly caused by contact angle hysteresis. Therefore, a low frequency signal at 1 kHz was applied on the square electrodes (1 mm × 1 mm) to increase the solid–liquid interaction forces by EWOD.[28,29] Moreover,

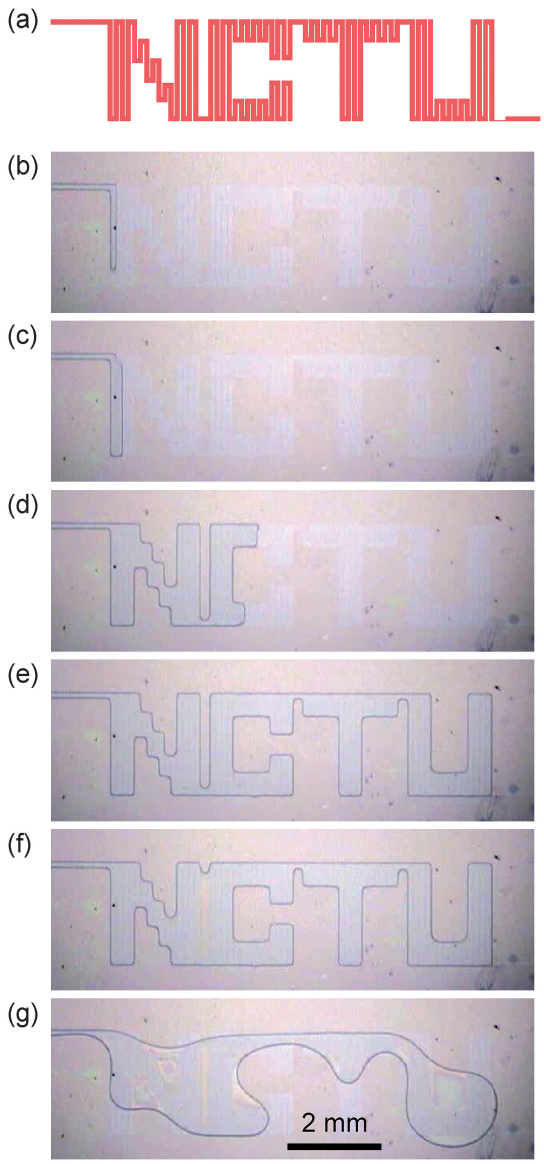

Fig. 4 Pumping liquid on a meandered electrode. (a) Meandered electrode design with the width of 100 μm and length of 112 mm. The spacing was 20 μm between the electrode within a single letter of "NCTU" and 200 μm between letters. (b) and (c) Increased channel width obtained by merging two water streams on an ITO electrode in a 25 μm high channel. The 20 μm spacing was spontaneously filled by capillarity because of the low liquid pressure from the Young–Laplace equation. (d) Division of the stream. (e) DEP pumping completed until the narrow region. (f) Capillary filling of the 200 μm spacing between "N" and "C". (g) Deformation and merging of water when no voltage was applied. Video 3 can be seen in the ESI.†

handling the reservoir by EWOD was helpful to perform the velocity experiments. For instance, EWOD was used to draw water pumped on the linear electrodes back to the reservoir electrode for the next experiment of different voltages on the same linear electrode. To test different linear electrodes with different widths, EWOD was applied to relocate the position of the reservoir by moving it upwards or downwards in the case shown in Fig. 2(a).

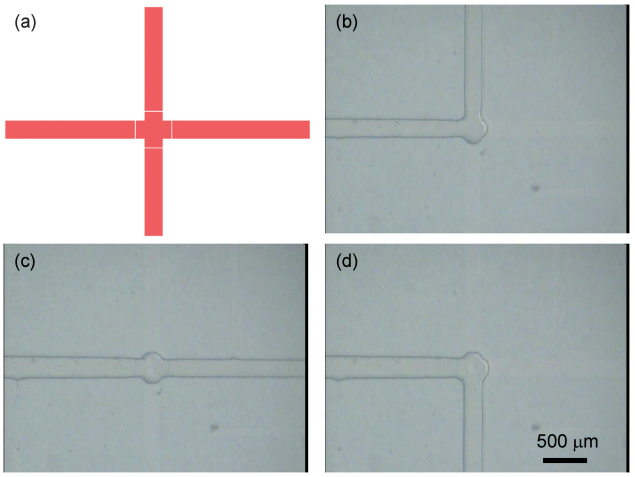

Fig. 5 Programmable crossing electrode set. (a) The electrode set consisted of a center crossing electrode and four linear electrodes. (b)–(d) The liquid was guided to different directions when the corresponding linear electrodes were energized.

Tapered and notched electrode (voltage-controlled valve)

The narrow region of the electrode worked as a flow stopper in the velocity experiments. However, water would pass this region if the applied voltage was sufficient, as can be seen in Video 1 in the ESI,† when voltage was increased above 125 Vrms. Therefore, an electrode with carefully designed width(s) would regulate the flow as a liquid valve by voltage applications.

The relation of the voltage and the electrode width was studied by a tapered electrode with a decreased width from 200 μm to 10 μm as shown in Fig. 3(a). Water was first placed and positioned on the reservoir electrode energized by a 1 kHz signal. A 100 kHz signal with various voltages was applied on the tapered electrode. Different channel heights, 50 and 25 μm, were examined. The minimum liquid width at varied applied voltage was measured. For example, as shown in Fig. 3(a), 90 μm was the recorded minimum width when 80 Vrms was applied in a 50 μm high channel. The measured minimum widths were converted to AR and plotted against the square of the applied voltage (V^2) in Fig. 3(b). It was found that the minimum AR was linearly proportional to V^2. The data in Fig. 3(b) can also be interpreted as the minimum required voltage to overcome a certain AR. A voltage-controlled valve was therefore implemented on a notched electrode indicated by the dashed lines in Fig. 3(c) and (d). As shown in Fig. 3(c), when the applied voltage was not sufficient, water was stopped before the notch where the AR was larger. Water passed the notch when adequate voltage was applied as shown in Fig. 3(d).

Meandered electrode (stability)

The stability of DEP pumping was demonstrated by a meandered electrode as shown in Fig. 4(a). The width and the length of the electrode before the narrow region at the lower right corner were 100 μm and 112 mm, respectively. The spacing between the meandered electrode was 20 μm within each letter of "NCTU" and 200 μm between letters. As water advanced along the electrode in a 25 μm high channel by applying 84 Vrms, the flow direction and the channel width were altered. As shown in Fig. 4(b) and (c), the

direction of the stream at the advancing tip was changed from downward to upward, and the width was increased from 100 μm (Fig. 4(b)) to 220 μm (Fig. 4(c)) when the 20 μm spacing was spontaneously filled with water. Because the liquid is pumped in a virtual microchannel defined by the electric field, combining multiple channels or pumping across different channels *in situ* is feasible with proper electrode designs and signal applications. Division of the stream was demonstrated in the letter "C" as shown in Fig. 4(d). Finally, water was pumped for 112 mm (Fig. 4(e)) and stopped before the narrow region of the electrode at the end of the letter "U". After water covered the four letters, the 200 μm gap between the letters "N" and "C" was gradually filled with water (Fig. 4(f)). It is noteworthy that because water was pumped in virtual microchannels without channel wall barriers, surface tension deformed and merged the pumped liquid when the DEP force was suddenly removed as shown in Fig. 4(g).

Particle solution was successfully driven on the meandered electrode as can be seen in Video 4 in the ESI.† The particle solution contained 5 μm polystyrene beads dispersed in water at the concentration of 4.2×10^8 particles ml^{-1}. Visualization of the liquid flow to comprehend DEP pumping is possible by observing the particles in the future. However, in the experiment, particles were not only moved by the liquid flow, but also by the DEP force exerting on the particles. In other words, the 100 kHz signal caused DEP on the pumped liquid as well as the suspended particles. As can be seen in Video 4 in the ESI,† particles were concentrated in the 20 μm spacing and the boundary of the liquid by negative DEP, which accorded with our previous studies and analyses.[28] The manipulation of particles by DEP in the virtual microchannel would be further developed to sort or concentrate particles along with the DEP pumped liquids.

Programmable crossing electrode set (reconfigurability)

In the above electrode designs, DEP liquid pumping was studied by a single electrode. When multiple discrete electrodes are used, more sophisticated liquid manipulations can be performed. For example, the liquid can be continuously pumped onto a discrete electrode to form a quantitative droplet after drawing the excess liquid back to the reservoir. We have successfully regulated the liquid in a continuous or discrete form by different electrode designs and electric signals on a single device, which will be reported elsewhere.

In addition, the reconfigurability can be demonstrated on multiple discrete electrodes. As shown in Fig. 5(a), a programmable crossing electrode set consisting of a center crossing electrode and four linear electrodes was designed. A four way switching valve was developed by selectively applying voltage on proper electrodes as shown in Fig. 5(b)–(d). A crossing virtual microchannel can be formed when all the five electrodes are energized. The investigated crossing electrode set would serve as a building block to construct a two-dimensional reconfigurable microfluidic network.

Discussion

Threshold voltage

Each curve in Fig. 2(b) exhibited a threshold voltage, V_T, to pump the liquid by DEP; meaning that threshold DEP forces were required to overcome certain resistance forces before pumping. It was found that curves with same AR presented similar V_T. In addition, although different AR needed different V_T, the calculated threshold DEP forces were similar (~2.9 μN from eqn (1)). In other words, the resistance forces in different experiments were similar and independent of the tested d and W. In our experiments, the volume of the reservoir was controlled to cover three square electrodes (Fig. 2(a)), hence the contour line length of the reservoir was the same. Therefore, the resistance force arose mainly from the solid–liquid interaction force, including surface tension and contact angle hysteresis, of the reservoir. The threshold voltage was increased when the EWOD voltage applied on the reservoir electrode was increased.

Similarly, the resistance force explains the relation between the applied voltage and the minimum liquid width studied by the tapered electrode. The DEP force generated on the tapered electrode balanced with a constant resistance force from the reservoir by assuming the decrease of the contour line length during experiment was negligible. Therefore, the square of the required voltage (V^2) was linearly proportional to AR (d/W) based on eqn (1). The curves of 25 and 50 μm high channels in Fig. 3(b) exhibited a similar slope because of the similar resistance force caused from a comparable contour line length of the reservoir.

Velocity

The pumping velocity achieved by applying voltage above V_T on the linear electrodes can be analyzed by the liquid pressure gradient derived from the interfacial pressure differences. When V_T was applied, the DEP force was about to overcome the resistance force; meanwhile, the liquid pressure, P_L, at the meniscus in the DEP electric field can be expressed as $P_M - \frac{\varepsilon_0(\varepsilon_L - \varepsilon_M)}{2d^2} V_T{}^2$ based on eqn (2). When the applied voltage V was increased over V_T, the liquid was pumped along the linear electrode by the P_L at the advancing meniscus, $P_M - \frac{\varepsilon_0(\varepsilon_L - \varepsilon_M)}{2d^2} V^2$. The liquid pressure gradient across the length of the virtual microchannel, l, was $\frac{\varepsilon_0(\varepsilon_L - \varepsilon_M)}{2ld^2}(V^2 - V_T{}^2)$. Therefore, the pumping velocity, proportional to the liquid pressure gradient, decreased as the liquid advanced along the electrode. The average pumping velocity over the length of the linear electrodes would be proportional to $V^2 - V_T{}^2$. As can be seen from Fig. 2(b), the pumping velocity in the electric-field-defined virtual microchannels can be controlled by the interfacial pressure difference. However, the interfacial pressure difference on surface-tension-defined virtual channel walls is constant during operation,[9] which is proportional to the channel height ($\Delta P \sim d^{-1}$) described by the Young–Laplace equation. In addition to the controllable pumping velocity, DEP would be more advantageous in liquid pumping as the channel height shrinks down because the interfacial pressure difference is inversely proportional to the square of the channel height ($\Delta P \sim d^{-2}$). Since the interfacial pressure difference is independent of W, pumping fluids in nanometre channels by DEP is theoretically feasible. In addition, concurrent liquid pumping in numerous channels of different widths at the same velocity is possible.

Continuous pumping

It may appear that the presented DEP actuation is not a continuous pumping mechanism. After forming a virtual microchannel,

pumping stops when the liquid reaches the end or the narrow portion of the powered electrodes. In fact, the liquid can be further pumped if another reservoir electrode is placed at the end of a DEP-formed microchannel to drain the liquid. With properly designed DEP electrodes, desirable liquid volume can be entirely pumped from a source reservoir electrode through the microchannel electrode to the drain reservoir electrode. However, if the volume exceeds what can be handled by DEP electrodes on a device of a reasonable size, other pumping mechanisms transporting liquid from inlet to outlet tubes attached to the device need to be considered. Nevertheless, DEP can still be used to form reconfigurable microchannels between the inlet and outlet.

Capillary filling

In the meandered electrode experiment, capillary filling was observed between wall-less virtual microchannels. Analogous to capillary rise, the filling process arose from the low liquid pressure at the meniscus in the spacing of the meandered electrode, which can be analyzed by the Young–Laplace equation $\Delta P = P_L - P_M = \gamma(1/R_1 + 1/R_2)$, where γ is the liquid–medium interfacial tension, and R_1 and R_2 are the principle radii of curvature. Because the meniscus at the filling interface contacted with identical liquid laterally, the contact angle was considered 0°. The radius of curvature on the plane horizontal to the parallel plates (top view) was negative (concave meniscus) and equalled to half of the spacing of the electrode s: $R_1 = -s/2$. The other radius of curvature on the plane vertical to the parallel plates (cross section) can be described as: $R_2 = -d/2\cos\theta_0$, where θ_0 is the contact angle of water on Teflon in oil. Because θ_0 was ~140° measured by the sessile drop method, the meniscus on the vertical plane was convex, and the value of R_2 was positive. The liquid pressures (P_L) at the menisci in 20 and 200 μm spacing were calculated as $P_M - 1546$ N m^{-2} and $P_M + 2053$ N m^{-2}, respectively. From the recorded video (Video 3 in the ESI†), P_L in the reservoir should be much higher than $P_M - 1546$ N m^{-2} because the 20 μm spacing was spontaneously filled (Fig. 4(c)) and slightly higher than $P_M + 2053$ N m^{-2} because fluctuation of the meniscus in the 200 μm spacing was observed before the whole meandered electrode was occupied by water. Continuously filling the 200 μm spacing started when DEP pumping stopped because the P_L at the meniscus of spacing held the lowest pressure in the liquid. The capillary filling can be controlled or prevented if the P_L in the reservoir is carefully managed. As can be seen in Video 5 in the ESI,† by increasing the EWOD voltage applied on the reservoir, the liquid filled in the 200 μm spacing was drained back to the reservoir. Capillary filling occurred again when the reservoir voltage was reduced.

Conclusions

We investigated liquids pumping in DEP-formed virtual microchannels on five electrode(s) patterns: linear, tapered, notched, meandered, and crossing electrodes, demonstrating the electric manipulations of continuous flow microfluidics. With proper voltage application, water was pumped at adjustable velocities (over 30 mm s^{-1}), in a microchannel of variable AR (0.1–2), or for a long distance (112 mm). Exploiting the linear relation of AR and V^2, voltage-controlled liquid valve was accomplished. On the other hand, liquid pumping between the virtual microchannels was demonstrated by capillary filling. DEP pumping is advantageous as the dimension of the liquid shrinks down because the interfacial pressure difference is proportional to the square of the electric field intensity and independent of the channel width. In addition, DEP-formed microchannels are free from dead volume and leakage, simplifying device fabrication and packaging. Liquid manipulation in and between the virtual microchannels increases the flexibility of microfluidics. The presented programmable crossing electrode set would realize a reconfigurable microfluidic network in the future.

Acknowledgements

This work is partially supported by National Science Council, Taiwan, R.O.C. under grants NSC 95-2221-E-009-266-MY3, NSC 97-2627-M-009-004, and NSC 97-2218-E-006-294.

References

1 T. M. Squires and S. R. Quake, *Rev. Mod. Phys.*, 2005, **77**, 977–1026.
2 G. M. Whitesides, *Nature*, 2006, **442**, 368–373.
3 H. Craighead, *Nature*, 2006, **442**, 387–393.
4 M. A. Burns, B. N. Johnson, S. N. Brahmasandra, K. Handique, J. R. Webster, M. Krishnan, T. S. Sammarco, P. M. Man, D. Jones, D. Heldsinger, C. H. Mastrangelo and D. T. Burke, *Science*, 1998, **282**, 484–487.
5 P. J. A. Kenis, R. F. Ismagilov and G. M. Whitesides, *Science*, 1999, **285**, 83–85.
6 M. A. Unger, H.-P. Chou, T. Thorsen, A. Scherer and S. R. Quake, *Science*, 2000, **288**, 113–116.
7 D. Jed Harrison, K. Fluri, K. Seiler, Z. Fan, C. S. Effenhauser and A. Manz, *Science*, 1993, **261**, 895–897.
8 R. B. M. Schasfoort, S. Schlautmann, J. Hendrikse and A. van der Berg, *Science*, 1999, **286**, 942–945.
9 B. Zhao, J. S. Moore and D. J. Beebe, *Science*, 2001, **291**, 1023–1026.
10 G.-B. Lee, B.-H. Hwei and G.-R. Huang, *J. Micromech. Microeng.*, 2001, **11**, 654–61.
11 S. K. Y. Tang, C. A. Stan and G. M. Whitesides, *Lab Chip*, 2008, **8**, 395–401.
12 H. A. Pohl, *Dielectrophoresis*, Cambridge University Press, New York, 1978.
13 L. Zheng, J. P. Brody and P. J. Burke, *Biosens. Bioelectron.*, 2004, **20**, 606–619.
14 K. D. Hermanson, S. O. Lumsdon, J. P. Williams, E. W. Kaler and O. D. Velev, *Science*, 2001, **294**, 1082–1086.
15 P. Y. Chiou, A. T. Ohta and M. C. Wu, *Nature*, 2005, **436**, 370–372.
16 J. A. Schwartz, J. V. Vykoukal and P. R. C. Gascoyne, *Lab Chip*, 2004, **4**, 11–17.
17 O. D. Velev, B. G. Prevo and K. H. Bhatt, *Nature*, 2003, **426**, 515–516.
18 H. Pellat, *C.R. Acad. Sci. Paris*, 1895, **119**, 691–694.
19 H. A. Haus and J. R. Melcher, *Electromagnetic Fields and Energy*, Prentice-Hall, Englewood Cliffs, 1989.
20 J. R. Melcher, D. S. Guttman and M. Hurwitz, *J. Spacecr. Rockets*, 1969, **6**, 25–32.
21 T. B. Jones, M. P. Perry and J. R. Melcher, *Science*, 1971, **174**, 1232–1233.
22 T. B. Jones and J. R. Melcher, *Phys. Fluids*, 1973, **16**, 393–400.
23 T. B. Jones, J. D. Fowler, Y. S. Chang and C.-J. Kim, *Langmuir*, 2003, **19**, 7646–7651.
24 T. B. Jones, K.-L. Wang and D.-J. Yao, *Langmuir*, 2004, **20**, 2813–2818.
25 K.-L. Wang and T. B. Jones, *J. Micromech. Microeng.*, 2004, **14**, 761–768.
26 T. B. Jones, M. Gunji, M. Washizu and M. J. Feldman, *J. Appl. Phys.*, 2001, **89**, 1441–1448.
27 R. Ahmed and T. B. Jones, *J. Micromech. Microeng.*, 2007, **17**, 1052–1058.
28 S.-K. Fan, P.-W. Huang, T.-T. Wang and Y.-H. Peng, *Lab Chip*, 2008, **8**, 1325–1331.
29 F. Mugele and J.-C. Baret, *J. Phys.: Comdens. Matter*, 2005, **17**, R705–R774.